Eur. Polym. J. Vol. 26, No. 9, pp. 1017–1025, 1990
Printed in Great Britain.

0014-3057/90 $3.00 + 0.00

BATCH EMULSION COPOLYMERS STYRENE WITH ETHYL ACRYLATE: MICROSTRUCTURE AND GLASS TRANSITION TEMPERATURE

S. DJEKHABA* and J. GUILLOT†
Laboratoire Des Matériaux Organiques, CNRS, B.P. 24, 69390 Vernaison, France

(*Received* 11 *December* 1989)

Abstract—Based on a previous kinetic investigation of batch emulsion copolymerization of styrene–ethyl acrylate (EA), the paper deals with experimental investigation on the copolymer microstructure (sequence distribution) and glass transition temperature. The DSC and NMR data are compared to theoretical quantities derived from a simulation taking into account monomer partition and polymer characteristics. Agreement between experiment and theory is fairly good; in particular the effect of difference of reactivity ratios which results in a huge composition drift for EA rich feeds, inducing a complex glass transition behaviour, is well accounted for. Comparison between experimental and theoretical (simulation) data could give useful indications of polymer compatibility.

INTRODUCTION

In a previous paper [1] the kinetics of emulsion copolymerization styrene–ethyl acrylate (S/EA) have been investigated, giving kinetic parameters ($r_{i,j}$, $kp_{i,j}$). In addition, this study showed that the occurrence of aqueous polymerization cannot be neglected. This paper deals with the microstructure of batch copolymers and its correlation with glass transition temperature, T_g. Recently, Johnston and Bassett reported experimental work on ^{13}C-NMR spectroscopy [2] and mechanical properties [3] of these copolymers, showing the large effect of the emulsion polymerization process, mainly the many structures and properties the so-called "power feed process" can allow. However, from our kinetic study, monomer partition has to be taken into account for the water solubility of EA is quite large; it is 26 g/l at 45°C [4], and the aqueous polymerization could reach up to 10% of total polymer, according to the experimental conditions. Owing to the reactivity ratios ($r_{EA} = 0.17$, $r_S = 0.9$) and the large difference in water solubility, the copolymer generated in the water phase is much richer in EA than the copolymer from particle polymerization. So, the final copolymer should be an "alloy" of polymers of different characteristics. It is expected that accurate ^{13}C-NMR and T_g investigations of batch copolymers isolated at various conversions can show the importance of the actual water polymerization and the composition drift caused by the difference in monomer reactivities. A simulation based on monomer partition coefficients, particle swelling and reactivity ratios can give a theoretical microstructure and its change as the reaction proceeds. It can also predict the glass transition behaviour. Indeed, it has been shown that T_g is closely related to the chain microstructure, above all the dyads (AA, AB, BB) distribution as shown in several recent approaches [5–7] and that the transition is spread over a temperature range which closely depends on the complexity of the mixture of macromolecules in the copolymer sample [8, 9].

EXPERIMENTAL PROCEDURES

A series of S/EA copolymers of various compositions have been prepared in emulsion in a batch reactor. Recipes are reported in Table 1. Polymerization technique and apparatus have been described [1].

Copolymer characterization

Copolymer chemical composition has been derived by several techniques:

- —monomer consumption was followed by gas chromatography (GC) analysis of withdrawn samples at various conversions;
- —elemental analysis (C, H, O) of flocculated, washed and dried samples;
- —^{1}H-NMR (Brucker WP 80) spectroscopy of copolymer samples in $CDCl_3$ solution.

Sequence distribution (microstructure) was determined by ^{13}C-NMR spectroscopy (Brucker WP 80, operating at 20.1 Hz with Fourier Transform) of copolymer samples as 5–20 wt% $CDCl_3$ solution, at 60°C with TMS as internal standard.

Glass transition temperature, T_g, were measured by Differential Thermal Analysis (SETARAM DSC 101) at a heating rate 10°C/min. The polymer sample was put in a pressure-sealed Al cell. The reference was an empty cell. The spectra were computerized.

Simulation of copolymer microstructure and T_g

The simulation program utilized for the kinetic investigation [1], based on monomer partition coefficients and polymer particle swelling [10], has been improved in order to compute the microstructure of instantaneous copolymer macromolecules. Indeed, in radical polymerization, the lifetime of a growing macroradical is very short (say msec to sec) before termination takes place; so the distribution of comonomer units along a macromolecule is like a

*Present address: Institut de Chimie U.S.T.H.B., B.P. 32, El Alia, Bab-Ezzouar, Alger, Algeria.
†To whom all correspondence should be addressed.

Table 1. S/EA—batch emulsion copolymerization, ^{13}C-NMR—comparison between theoretical and experimental data for mole percent of monomer units centered in various triads

	Conversion %	AAA	AAS	SAS	SSS	SSA	ASA
(1) $(AE/S)_0 = 80/20$; M/W = 0.2							
Experimental	12.8	12.5	48	39.5	0	36	64
Simulated	12.7	14.6	46.1	39.3	4.3	33.1	62.6
Experimental	54.8	25.5	51	23.5	2	30.5	67.5
Simulated	58.3	33.4	44.4	22.2	2.3	24.6	73.1
Experimental	98	65	28	7	2.5	19	78.5
Simulated	98	64.8	24.5	10.7	2.3	23.1	74.5
(2) $(AE/S)_0 = 50/50$; M/W = 0.2							
Experimental	16.6	0	17	83	26.5	54.5	19
Simulated	12.6	2.5	21.4	76.1	27.6	50	22.4
Experimental	50.9	0	25.5	74.5	23	55.5	21.5
Simulated	49.3	2.2	23.8	74	24.1	49.5	25.4
Experimental	97.7	16	35	49	15	50.5	34.5
Simulated	97.1	18.5	30.3	51.2	16.2	45	38.8
(3) $(AE/S)_0 = 20/80$; M/W = 0.2							
Experimental	19.7	0	10	90	65.5	29.5	5
Simulated	22.9	0	6.2	93.8	66.4	30	3.6
Experimental	50	0	10	90	67	27	6
Simulated	49.3	0	7.3	92.7	65.6	30.6	3.8
Experimental	96.6	0	9.5	90.5	62.7	31	6.3
Simulated	97.1	0	8.7	91.3	61.6	33.6	4.8

"fingerprint" of the monomer feed at the given time and locus where this molecule has been generated. As a consequence, only the individual, i.e. instantaneous, macromolecules, have a physical meaning, and the final product is a mixture of macromolecules whose microstructure distribution is more or less complex according to the composition drift during the copolymerization.

Unfortunately, the usual analytical techniques (NMR, i.r. elementary analysis) cannot see individual molecules but only an overall (mean) copolymer. However recently, German and co-workers [11, 12] have used combined size exclusion chromatography (SEC) and quantitative thin layer chromatography (TLC, FID) to characterize the macromolecular microstructure of methyl acrylate/S copolymers; they have obtained the molar mass distribution in relation with chemical composition at the specific molar mass (MMCCD) and the triad fractions and tacticity parameters of copolymers.

Theoretically, the derivative of an experimental curve with respect to the conversion, for instance, should give the instantaneous value but usually at low accuracy. Another way, more commonly used, is to compute the sequence distribution (microstructure) from the theory of copolymerization [13, 14] for a very small conversion increment and by numerical integration to compute the mean values. If several polymerization loci exist, as expected for the emulsion copolymerization under investigation, integration done for each site and a global microstructure is derived. For NMR, the computations have been limited to the dyads (AA, AB, BB) and triads (AAA, AAB, BAB, BBB, BBA, ABA) and fraction of units centred in given triads whose resonances are easily assigned. For T_g, the simulation is more sophisticated and quite original. It is considered that instantaneous copolymer T_g can be calculated from the dyad (I.J) and associated T_g ($T_{g_{ij}}$). The many instantaneous macromolecules are, then, classified in groups of molecules having the same T_g within, for instance, 1 K. At a selected conversion each group is weighted and the mean heat capacity (C_p) of the whole copolymer sample is computed for any temperature, taking into account the weight of polymer already above the transition temperature (C_{p_l}) and the weight of polymer still in the glassy state (C_{p_s}) at the temperature [8].

NMR spectroscopy (^{1}H and ^{13}C)

The kinetic investigation of batch S/EA copolymerization in the previous paper [1], mainly based on GC analysis of the unreacted monomers at various times (conversions), indicated a water copolymerization with importance increasing with dilution [decreasing monomer/water (M/W) ratios], along with the polymer particle polymerization. NMR spectroscopy has been performed with two main objectives:

—^{1}H-NMR to investigate copolymer composition changes for the resulting copolymers (and not on residual monomers); i.e. to verify the conclusion of the GC method;

—^{13}C-NMR to determine the sequence distribution (microstructure) of copolymer samples withdrawn at various conversions and initial experimental conditions (M/W), in order to check the theoretical microstructure computed by a simulation program developed from the kinetic study and to know to what extent the aqueous copolymer modifies the NMR microstructure pattern, as would be expected, from simple bulk or solution copolymerization.

(A) ^{1}H-NMR spectroscopy: the proton resonance is known to be safer for quantitative analysis of copolymer composition which needs to compare resonance of various kinds of atoms. In this study several groups of protons have been used (Fig. 1) mainly according to the copolymer composition: phenyl ring protons (S_1) can be compared to the methoxy protons —O—CH_2—(S_2) or to other protons (S_3), according to the following equations:

$$\text{Molar fraction of EA} = \frac{S_2/2}{S_2/2 + S_1/5}$$

or

$$EA = \frac{5S_3 - 3S_1}{5S_3 + 3S_1}.$$

Data derived from ^{1}H-NMR and elemental analysis are in quite good agreement with the simulation taking into account the aqueous polymerization (Fig. 2); the simulation has been improved over that used in the previous paper [1].

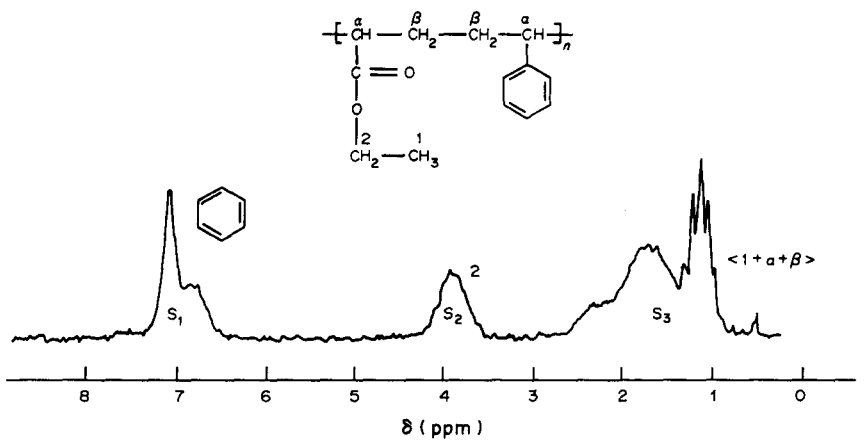

Fig. 1. S/EA batch emulsion copolymerization ^{1}H-NMR spectrum (80 MHz) of copolymer with 60 mol% EA.

Indeed, based an experimental data, an enhanced water solubility of S, induced by increasing EA contents in the initial monomer feed, is taken into account. Such effect of polar monomers has already been observed for methyl acrylate [15] and acrylonitrile [16], for instance.

This good agreement between experiment and theory confirms clearly the predominance of EA rich copolymer chain at low conversion ($\leqslant 20\%$). As conversion increases, the main polymerization locus becomes the usual polymer particle phase and copolymer composition becomes closer (within experimental error) to the composition computed by the program not taking account of polymerization in the water phase. Samples for ^{1}H-NMR analysis have been precipitated, washed and dried, which means that their molecular weights are not too low; it is even thought it could be large enough to be chains or long chains segments. If one can reasonably trust the simulation, the water copolymer is very enriched in EA.

For $(F_{EA})_O = 0.80$, $(F_{EA})_W = 0.98$ at M/W = 0.2

$(F_{EA})_O = 0.5$, $(F_{EA})_W = 0.94$ at M/W = 0.2

$(F_{EA})_O = 0.2$, $(F_{EA})_W = 0.8$ at M/W = 0.2

where $(F_{EA})_O$, $(F_{EA})_W$ refers to mol fraction of EA in organic and water phases, respectively; similar values at M/W = 0.5 are observed.

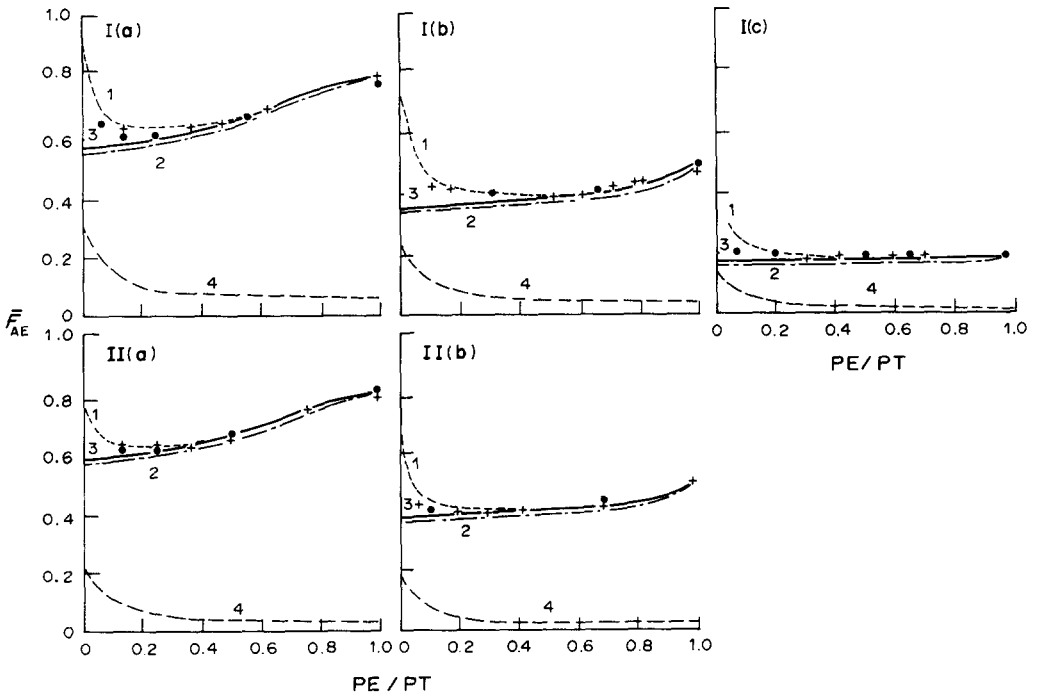

Fig. 2. S/EA batch emulsion copolymerization effects of dilution (M/W) and monomer feed composition on copolymer composition (mean mole fraction $\bar{F}_{EA}$) I, M/W = 0.2; II, M/W = 0.5. Initial monomer feed: (a) 80 mol% EA; (b) 50 mol% EA; (c) 20 mol% EA. Simulation with water polymerization: overall mean copolymer chemical composition (1); mean copolymer chemical composition within particles (2). Simulation neglecting water polymerization: overall mean copolymer chemical composition (3). Experimental data: GC (●); ^{1}H-NMR and elemental analysis (+); water polymerization/total polymer (4).

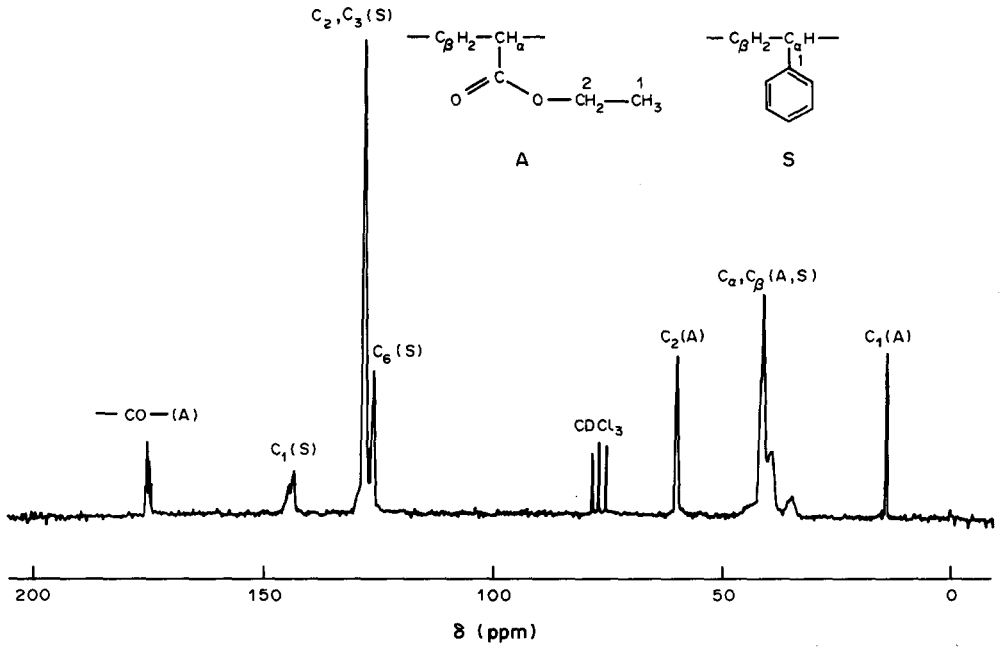

Fig. 3. S/EA batch emulsion copolymerization ^{13}C-NMR spectrum (20.1 MHz) of copolymer with 50 mol% EA.

The proportions of aqueous copolymer in the overall copolymer are reported in Fig. 2, vs conversion. As expected, its effect is more marked at high EA content and lower M/W. The main conclusion from this copolymer composition study is, doubtless, that an emulsion EA/S copolymer is heterogeneous: along with the copolymer generated within the polymer particles, EA rich copolymer is formed in the water phase, in amount not negligible at low conversion, at high EA content in the initial monomer feed and at high dilution (low M/W ratio).

In addition, in a batch process, the usual monomer composition drift is to be added. As a consequence a more complex sequence distribution analysis should be expected as well as a more complex behaviour of properties chiefly dependent on microstructure, such as T_g.

(B) ^{13}C-NMR spectroscopy: Johnston and Bassett have published a detailed ^{13}C-NMR study of a series of EA/S

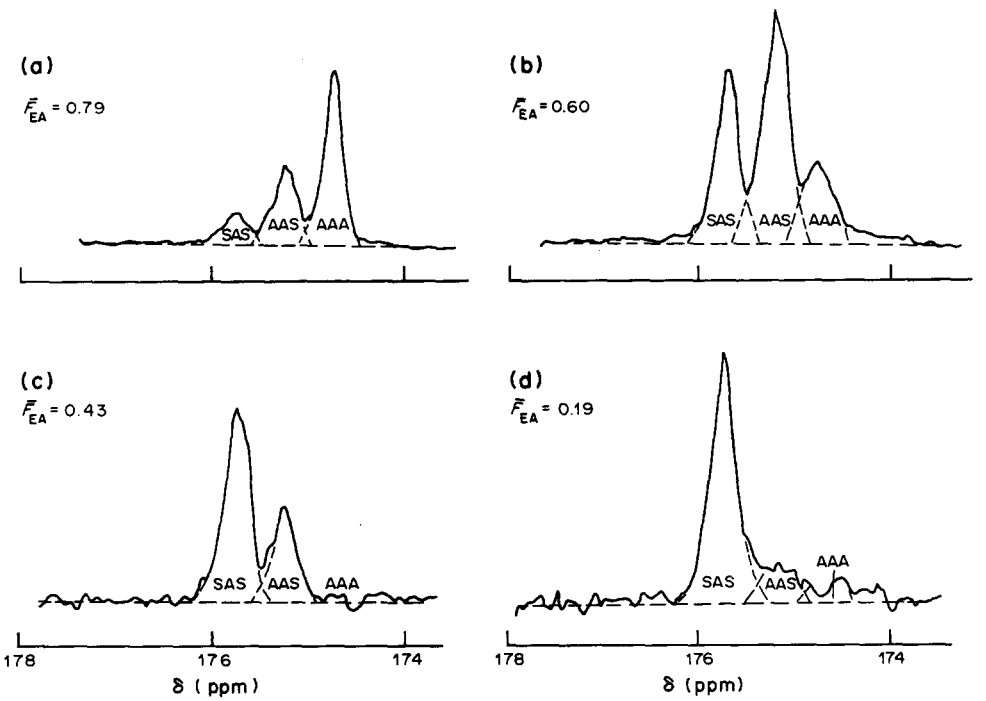

Fig. 4. S/EA batch emulsion copolymerization expanded ^{13}C-RMN spectra (20.1 MHz) of the carbonyl carbon resonance region of copolymers with various mol% EA (F_{EA}).

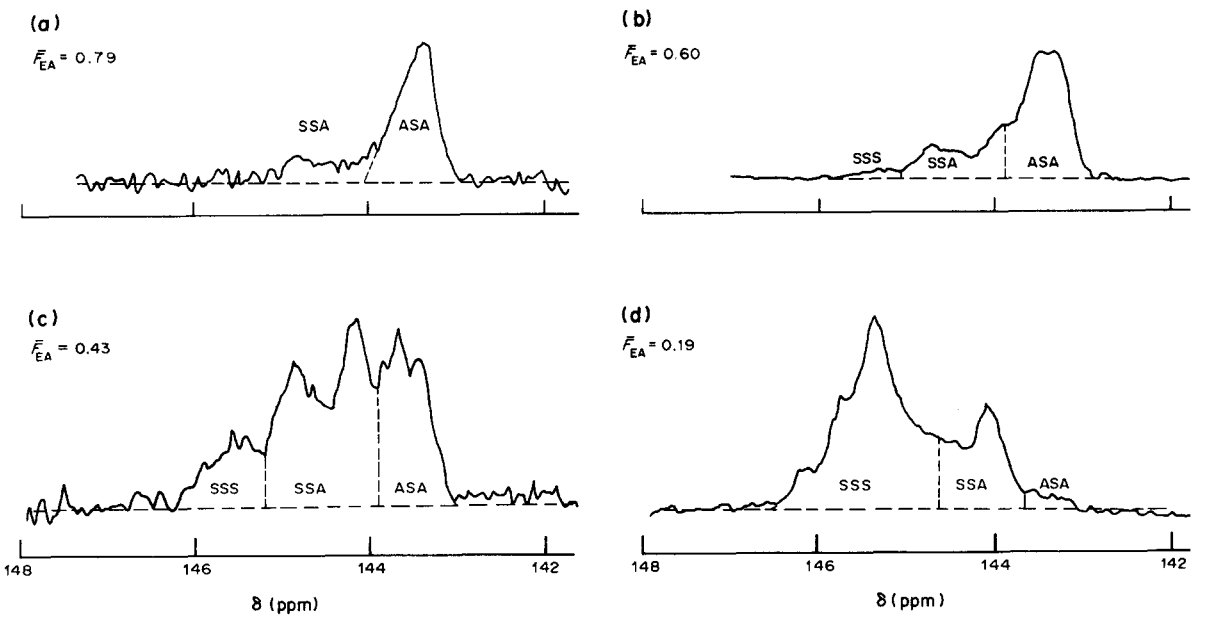

Fig. 5. S/EA batch emulsion copolymerization expanded ^{13}C-NMR spectra (20.1 MHz) of the quaternary carbon C_1(S) resonance region of copolymer with various mol% EA (F_{EA}).

copolymers [2] prepared by their quite new "power feed" process which allows the distribution of copolymer chain microstructure to be tailored. Their main objective was to use triad distribution data to derive reactivity ratios by the Harwood "run number" treatment. Assignments proposed can be considered as correct since $r_{i,j}$ values are in the expected range, despite a quite large standard deviation. As mentioned recently [17], quantitative data can be derived for different alkyl length pendant group relaxation, but with an accuracy decreasing as the length of the alkyl group increases. However, in the computation, they did not take account of the aqueous polymerization. Quantitative determination have been done on the carbonyl carbon of the acrylate and the phenyl C_1 of S (Fig. 3). Figures 4 and 5 report some spectra and show the change as composition varies. The accuracy in triad analysis is not very high owing to a rather bad signal-to-noise ratio. This is particularly the case at low EA content, for long EA sequence (AAA). It is also worthy of mention that the partition proposed for S centred triads (Fig. 5) could be doubtful. Data by planimetry are reported in Table 1.

T_g: it is still usual to predict copolymer T_gs with the Fox equation (18):

$$1/T_g = W_A/T_{g_A} + W_B/T_{g_B}$$

where W_i, T_{g_i} refer to weight fraction and T_g of monomer i. However, experiment shows that in many cases, large deviations are observed, particularly with acrylate copolymers. It is now believed that T_g is related not to the overall chemical composition but to dyad distribution of the copolymer. Many equations have been proposed which relate the copolymer to the dyads AA, AB, BB and T_g of pure "Parent" homopolymers and T_g of an ideally alternating AB copolymer. The weighting factor changes from one author to another, for instance: the weight fraction for Johnston [5], rotatable bonds in the dyads for Barton [6] or, better, the increment of heat capacity when passing from solid state to liquid state at the T_g associated with each dyad, for Couchman [7].

Johnston's equation:

$$1/T_g = W_A P_{AA}/T_{g_A} + W_B P_{BB}/T_{g_B} + (W_A P_{AB} + W_B P_{BA})/T_{g_{AB}}.$$

Where P_{ij} are the conditional probabilities and are expressed, as:

$$P_{AB} = 1/(1 + r_A[A]/[B]) = 1 - P_{AA}$$

$$P_{BA} = 1/(1 + r_B[B]/[A]) = 1 - P_{BB}$$

r_A, r_B are reactivity ratios; [A], [B] are monomer concentrations.

Barton's equation:

$$T_g = n'_{AA} T_{g_A} + n'_{BB} T_{g_B} + (n'_{AB} + n'_{BA})(T_{g_{AB}})$$

where

$$n'_{ij} = (n_{ij}\alpha_{ij})/(\Sigma n_{ij}\alpha_{ij})$$

where a_{ij} is the number of rotatable bonds for atom group in the dyad ij having n_{ij} distribution.

Couchman's equation:

$$\ln T_g = \frac{n_{AA}\Delta C_{p_A} \ln T_{g_A} + n_{AB}\Delta C_{p_{AB}} \ln T_{g_{AB}} + n_{BB}\Delta C_{p_B} \ln T_{g_B}}{n_{AA}\Delta C_{p_A} + n_{AB}\Delta C_{p_{AB}} + n_{BB}\Delta C_{p_B}}$$

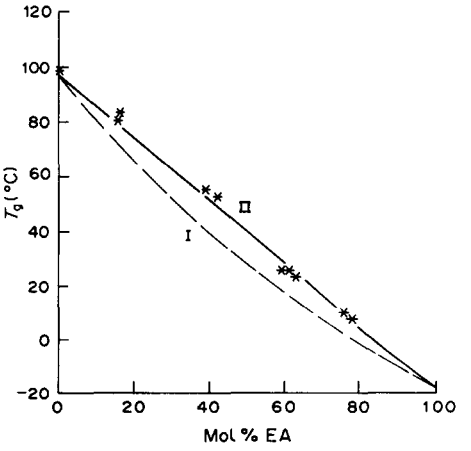

Fig. 6. S/EA batch emulsion copolymerization T_g, as a function of homogeneous copolymer composition. I, Johnston equation; II, Fox equation. *Experimental data (DSC at 10°C/min).

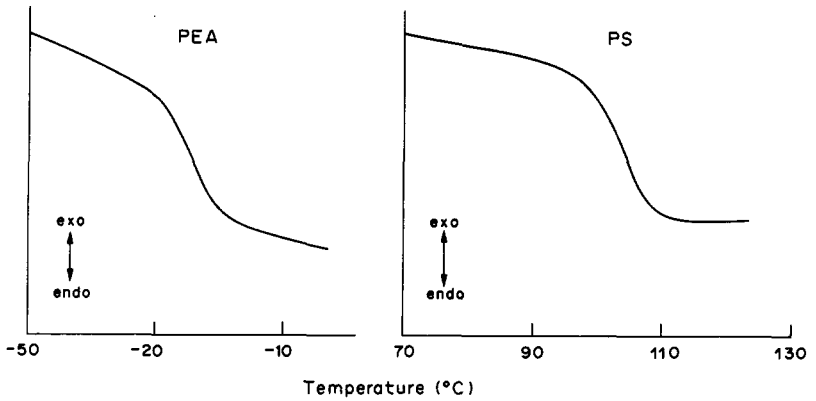

Fig. 7. S/EA batch emulsion copolymerization DSC curves of PS (m = 83.3 mg) and PEA (m = 83 mg); heating rate 10°C/min, sensitivity 50 mv.

where $\Delta C_{p_i} = C_{p_i^s} - C_{p_i^l}$ for dyad ii and expressing of molar fraction n_{ij} of dyad ij are:

$$n_{AA} = P_{AB}P_{AA}/(P_{AB} + P_{BA})$$

$$n_{BB} = P_{AB}P_{BB}/(P_{AB} + P_{BA})$$

$$n_{BA} = n_{AB} = P_{BB}P_{AA}/(P_{AB} + P_{BA}).$$

Owing to the number of parameters (three at least), all these equations can fit the experimental curves. Unfortunately it is not usually possible to synthesize a true alternating copolymer. However, a good estimate of $T_{g_{AB}}$ can be the T_gs of the more statistical copolymer of the series under investigation; i.e. the 50/50 molar for which (AB) is maximum. So the value of $T_{g_{AB}}$ which allows the best fitting can change a little from one equation to another. In addition in the most attractive Couchman's equation, additional parameters are the heat capacity increments which are not always known with accuracy, particularly for the alternating copolymer. So, in this work the Johnston equation is used with a $T_{g_{AB}}$ assumed to be $T_{g_{SAE}} = 317$ K ($T_{g_{AE}} = 255$ K, $T_{g_S} = 371$ K), (Fig. 6). To minimize the number of parameters, the overall heat capacity of a copolymer sample is calculated at any temperature according to a simple

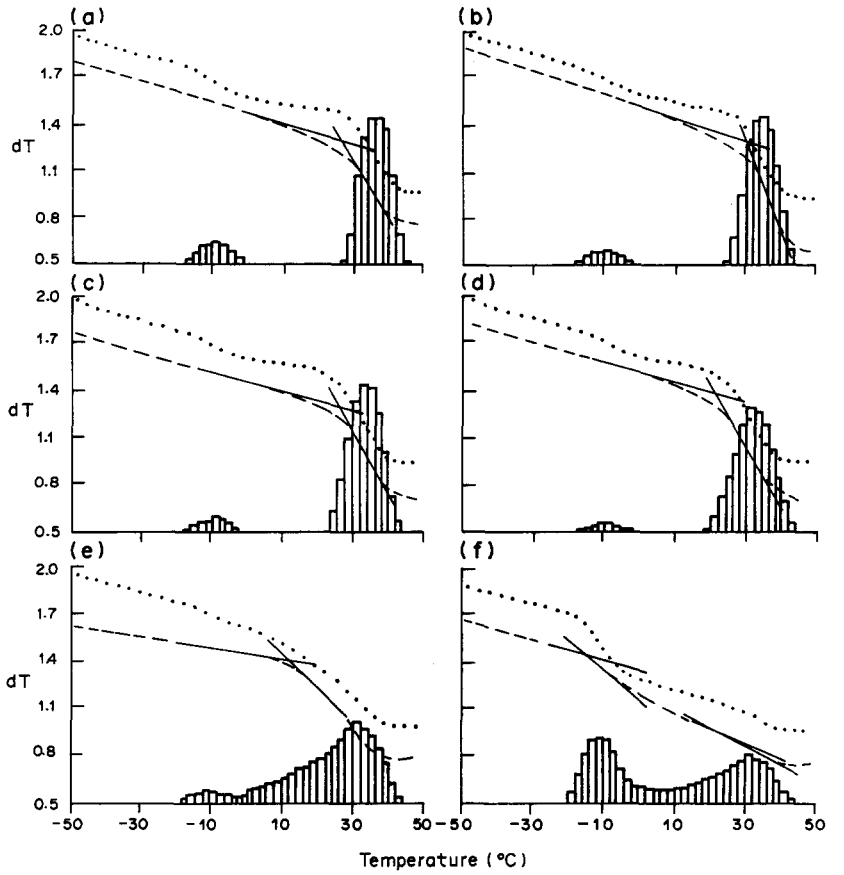

Fig. 8. S/EA batch emulsion copolymerization DSC curves and histograms. Initial monomer feed: 80 mol% EA; M/W = 0.2. Overall conversion, simulation (· · ·): (a) 6.8%; (b) 13%; (c) 21.7%; (d) 31.1%; (e) 56.5%; (f)98%. Experimental data (----): (a) 4.8%; (b) 13%; (c) 23.6%; (d) 35.4%; (e) 54.8%; (f) 98%.

additional rule from heat capacity data at 298 K given in the literature [19], for both S and EA homopolymers:

$$C_{p_S^l} = 1720\ \text{j/kg·K} \qquad C_{p_S^g} = 1220\ \text{j/kg·K}$$

$$C_{p_{EA}^l} = 1820\ \text{j/kg·K} \qquad C_{p_{EA}^g} = 1450\ \text{j/kg·K}.$$

The simulation takes account also of the change of C_p with temperature [19]. As it is observed that the glass transition of a homopolymer is spread over few Kelvin, the program includes an additional distribution derived from experimental DSC curves for both PS and PEA homopolymers (Fig. 7) at the same heating rate (10 K/min). For easier discussion, the theoretical DSC curves and histogram (i.e. the weight percent of copolymer chains with the same T_g within ± 1 K) have been plotted on the same figures, along with the experimental curve.

The kinetic study [1] has confirmed the difference between the reactivity ratios ($r_S = 0.92$, $r_{AE} = 0.17$); it should result in a large composition drift of the instantaneous monomer mixture in a batch reactor. Hence, according to the radical polymerization characteristics, the distribution of the instantaneous (individual) copolymer chain microstructure (sequence distribution) is wider when the initial S content is smaller in the monomer feed with, in addition, an enhanced effect at lower M/W ratios (lower solid content). Figures 8–10 report theoretical histograms and DSC curves and experimental DSC curves for various initial monomer feeds at two M/W ratios (0.2 and 0.5).

Agreement is quite fair between experimental DSC data and the theoretical DSC curves. At high S content, a marked skewing towards lower temperature is observed on theoretical as well as on experimental curves. It is closely related to the monomer feed drift which results in macromolecules richer and richer in EA, the less reactive monomer; hence it results in molecules of lower and lower T_gs. This skewing is less marked at an initial 50/50 mol/mol feed and practically not seen at higher S content (20/80 mol/mol). As a matter of fact, from the kinetic investigation [1] in this composition range, quasi-azeotropic copolymers are expected, i.e. copolymers without significant composition drift, up to high conversion.

The changes in the shape of the curves seem to be well matched by the simulation of the T_gs for the main transition.

It is noteworthy that good agreement exists between experimental and theoretical thermograms at high conversion for the EA 80 mol% sample, prepared for both M/W ratios (0.2 and 0.5); this corresponds to a huge composition drift.

The small transition predicted by the simulation at low temperature, which is assigned to macromolecular chains generated in the water phase, is not experimentally discernible at low conversions for copolymers prepared with EA rich (80 mol%) monomer feeds, and for which a rather high contribution of water polymerization (10–15% of total polymer) would be expected. However, a shift towards lower temperatures is observed at the beginning of the main transition range for S rich copolymers, particularly at low conversion (Fig. 9). An explanation could be a plastification effect of S rich macromolecules, prevailing at the beginning of batch polymerization, by the rich EA chain from the water phase. As a result the transition of the latter would be shifted to higher temperature and T_gs of the former would be shifted towards lower temperature. As the

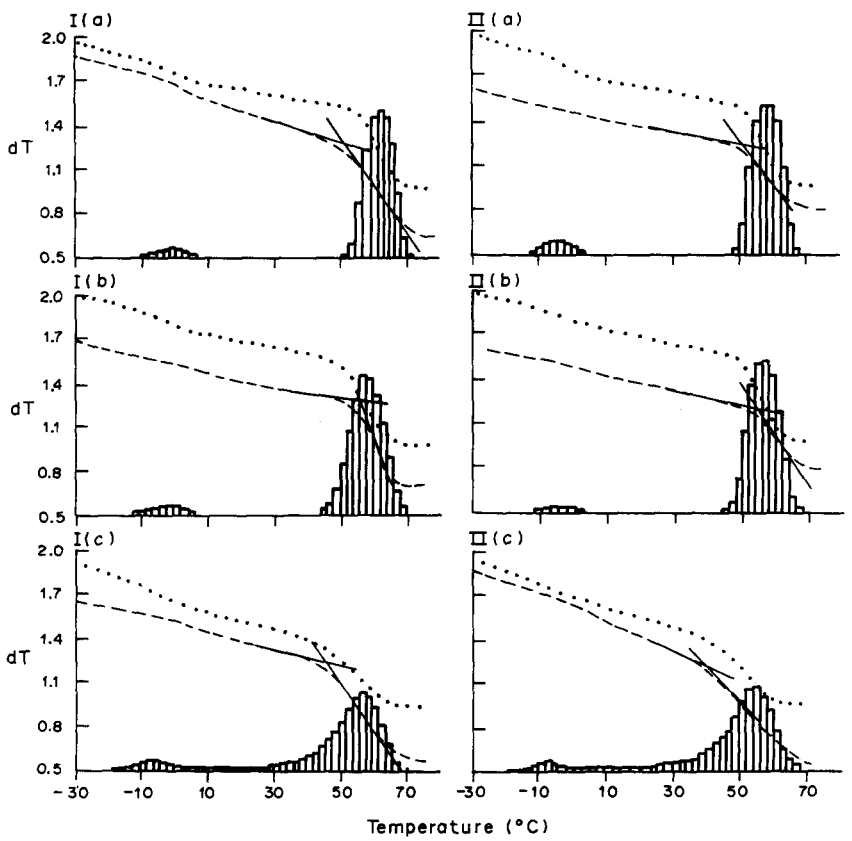

Fig. 9. S/EA batch emulsion copolymerization DSC curves and histograms. Initial monomer feed: 50 mol% EA. I, M/W = 0.2; overall mol conversion, simulation (· · ·): (a) 10.7%; (b) 51.7%; (c) 98%. Experimental data (———): (a) 10.8%; (b) 50%; (c) 99%. II, M/W = 0.5, simulation (· · ·): (a) 6.2%; (b) 39.2%; (c) 98%. Experimental data (———): (a) 5.0%; (b) 41%; (c) 98%.

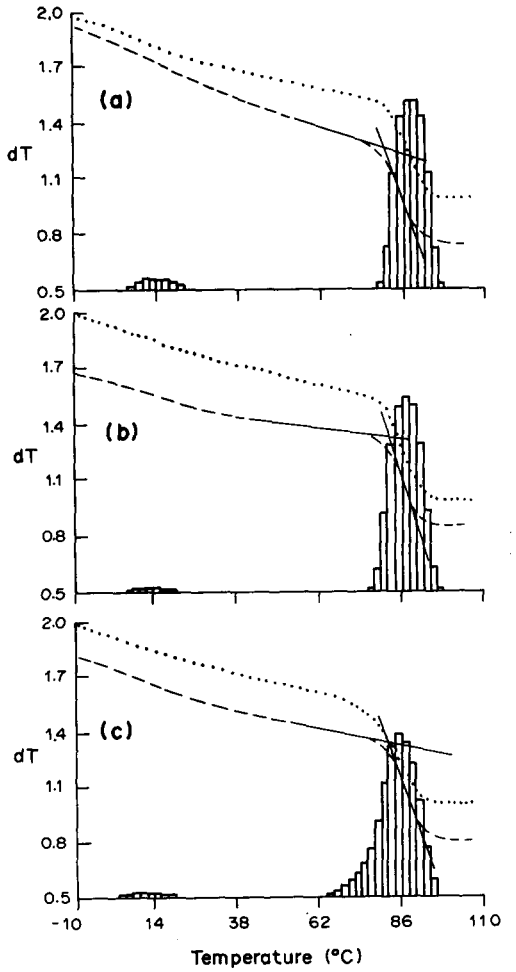

Fig. 10. S/EA batch emulsion copolymerization DSC curves and histograms. Initial monomer feed: 20 mol% EA; M/W = 0.2. Overall conversion, simulation (···): (a) 6.6%; (b) 51.7%; (c) 98%. Experimental data (———): (a) 7.2%; (b) 49; (c) 97.

conversion increases, the amount of particle copolymers prevails and progressively the water copolymer is rejected by S rich chain (phase separation ?) in more isolated domains in the film sample. That effect suggests a limited compatibility between PS and PEA.

CONCLUSION

The fair agreement between experimental and simulated data shows that it is possible to model the copolymerization mechanism with accuracy and to derive reliable quantitative data on kinetics and microstructural characteristics of the resulting macromolecules. However, ^{13}C-NMR and DSC do not put directly indicate the occurrence of aqueous generated copolymers. This could be due to the lower sensitivity of ^{13}C-NMR for quantitative analysis; indeed in an artificial mixture of homogeneous S/EA copolymer with 10% of pure EA homopolymer, the ^{13}C-NMR analysis does not show significant modification of the spectrum by comparison with that of a batch copolymer with the same overall chemical composition.

A more interesting aspect, perhaps, of the close correlation between simulation and experiment of the glass transition behaviour is that it could be an indirect way to obtain information on particle structure and polymer compatibility. Indeed, simulation of copolymer T_gs is based on the assumption that any copolymer macromolecule keeps its own T_g—determined by its microstructure (dyad distribution)—in the complex polymer chain mixture in a sample withdrawn from the emulsion at various conversions. In other words, when there is no deviation between modelled T_g and experimental DSC thermograms, it could be inferred that a copolymer macromolecule is located in a domain with only very similar macromolecules, i.e. there is practically no mixing with polymer chains of different composition or microstructure for, in that case, the T_gs would have rather more followed the Fox equation. So, according to the chemical shift induced by the process and the reactivity ratios, copolymer molecules are gathered in domains of quite similar glass transition behaviour; a compositional gradient is therefore expected within the particle, which is also evidence of the poor compatibility of macromolecules of different composition. A consequence of the bad copolymer mixing is that the chemical composition of the particle surface should change with conversion and initial feed composition. The soap adsorption technique of Maron [20] to measure the polarity of the particle surface confirms quite well the assumption of a chemical gradient for a suitable co-monomer system (specific area occupied by SDS emulsifier molecule is: $A_S(S) \pm 52$ Å^2 and $A_S(EA) \pm 115$ Å^2. A large chemical shift in batch emulsion is observed for EA rich feed and results in EA monomer accumulation at high conversion, i.e. in particle surface richer and richer in EA monomer and hence in A_S closer and closer to A_S(EA). Figure 11 which reports data on A_S measurements by the Maron method seems to confirm the particle structure.

Thus it seems that something close to phase separation occurs during batch emulsion copolymerization of S and EA resulting in particle structure. If there is some compatibility deviation should be expected

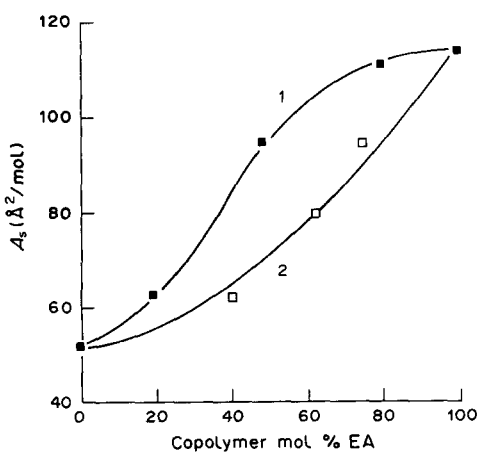

Fig. 11. S/EA batch emulsion copolymerization variation of molecular surface area (A_S) of SDS with copolymer composition. (1) Batch; (2) composition controlled-Batch.

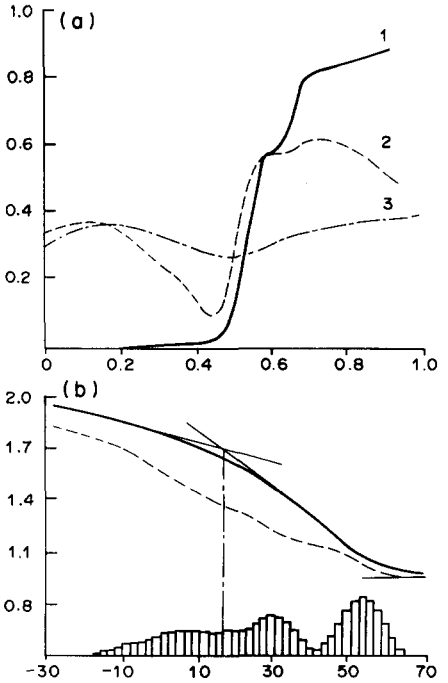

Fig. 12. S/EA emulsion copolymerization badly controlled "corrected batch" process. (a) Kinetic curves showing the way S has been added: 1, rate of addition S monomer; 2, instantaneous copolymer composition (F_S); 3, overall mean copolymer composition ($\bar{F}_S$). (b) DSC curves and histograms of final sample, at 92% molar conversion: simulation (– – –); experimental data (——).

between theoretical and experimental DSC thermograms. This is indeed observed, when a complex polymerization process in used leading to better mixing of copolymer chains, as in some badly controlled "corrected batch" syntheses. Figure 12 shows a huge deviation between theory and experimental data which corresponds rather more to the Fox equation.

Accurate kinetic investigation of batch emulsion S/EA copolymerization allowed to derive reliable model and computer simulation of the microstructure and glass transition behaviour. The deviation between experimental and theoretical DSC thermogram and histogram can even lead, to some extent at least, to better knowledge of particle structure and polymer compatibility.

Acknowledgement—The authors are indebted to Mrs Christiane Monnet for carrying out the NMR spectra analysis and for fruitful discussions.

REFERENCES

1. S. Djekhaba, C. Graillat and J. Guillot. *Eur. Polym. J.* **24,** 109 (1988).
2. J. E. Johnston, D. R. Bassett, T. B. MaCrudy. In *Emulsion Polymer and Emulsion Polymerization* (edited by D. R. Bassett and H. E. Hamielec), p. 389. ACS Symposium Series 165 (1981).
3. D. R. Bassett and K. L. Hoy. In *Emulsion Polymer and Emulsion Polymerization* (edited by D. R. Bassett and H. E. Hamielec), p. 371. ACS Symposium Series 165 (1981).
4. V. I. Eliseeva. In *Emulsion Polymerization and its Application in Industry*. Plenum, New York (1981).
5. N. Johnston. *Am. Chem. Soc.; Polym. Prepr.* **14,** 46 (1973).
6. J. Barton. *J. Polym. Sci.; Part C,* **30,** 573 (1970).
7. P. R. Couchman. *Macromolecules* **15,** 3 (1983).
8. J. Guillot and B. Emelie. *XV^e cong., AFTPV, Cannes* 179 (1983).
9. J. Guillot and W. Ramirez. *IUPAC Symposium, Genoa, Italy*. p. 170 (1987).
10. J. Guillot. *Makromolek. Chem., Suppl.* **10/11,** 253 (1985).
11. G. H. J. Van Doremaele and A. L. German. *2^e colloque international sur les copolymères en milieu dispersé, Lyon, France*, Prepr. p. 63 (1989).
12. G. H. J. Van Doremaele, J. C. Ammerdorffer, A. M. Van Herk and A. L. German. *Polym. Comm.* **29,** 299 (1988).
13. K. Ito and Y. Yamashita. *J. Polym. Sci.* **A-3,** 2165 (1965).
14. C. W. Pyun. *J. Polym. Sci.* **23,** 733 (1979).
15. W. Ramirez and J. Guillot. *Makromolek. Chem.* **189,** 379 (1988).
16. I. Capek, J. Barton and E. Orolinova. *Acta Polym.* **36,** 187 (1985).
17. M. F. Llauro, C. Pichot, W. Ramirez-Marquez and J. Guillot. *Am. Chem. Soc.* **54,** 613 (1988).
18. T. Fox. *Bull. Am. Phys. Soc.* **1,** 123 (1956).
19. D. N. Van Krevelen. *Properties of Polymers*, 2nd Edn, pp. 81–89 (1976).
20. S. H. Maron, M. E. Elder et I. N. Ulevitch. *J. Colloid Sci.* **9,** 89 (1954).